1 Method

1.1 Maxwell's Equations Governing the Mode

Starting from Maxwell's curl equations,

$$\nabla \times \mathbf{E} = -\frac{\partial \mathbf{B}}{\partial t} \tag{1a}$$

$$\nabla \times \mathbf{H} = \frac{\partial \mathbf{D}}{\partial t} \tag{1b}$$

where electric field intensity $\mathbf{E}$ and electric field density $\mathbf{D}$, magnetic field intensity $\mathbf{H}$ and magnetic field intensity $\mathbf{B}$ are related by constitutive equations

$$\mathbf{B} = \mu_0 \mathbf{H} \tag{2a}$$

$$\mathbf{D} = \epsilon_0 [\epsilon_r] \mathbf{E} \tag{2b}$$

where material is considered to be linear, electrically anisotropic, nonmagnetic and nondispersive. Scalar μ_0 and ϵ_0 are permeability and permittivity in free space and tensor quantity $[\epsilon_r]$ is the relative permittivity for anisotropic materials and

$$[\epsilon] = \epsilon_0 [\epsilon_r] = \epsilon_0 \begin{bmatrix} \epsilon_{xx} & \epsilon_{xy} & 0 \\ \epsilon_{yx} & \epsilon_{yy} & 0 \\ 0 & 0 & \epsilon_{zz} \end{bmatrix} \tag{3}$$

where a three dimensional right-handed Cartesian coordinate system x, y, z is assumed.

Assume all field quantities have a time dependence of $e^{j\omega t}$ and convert (1) into frequency domain,

$$\nabla \times \mathbf{E} = -j\omega \mathbf{B} = -j\omega \mu_0 \mathbf{H} \tag{4a}$$

$$\nabla \times \mathbf{H} = j\omega \mathbf{D} = j\omega \epsilon_0 [\epsilon_r] \mathbf{E} \tag{4b}$$

Combining frequency-domain curl equations (4),

$$\nabla \times ([\epsilon_r]^{-1} \nabla \times \mathbf{H}) = \omega^2 \mu_0 \epsilon_0 \mathbf{H} = k^2 \mathbf{H} \tag{5}$$

Assume all field quantities have a z dependence of $e^{-j\beta z}$, $[\epsilon_r]^{-1} \nabla \times \mathbf{H}$ in

(5) can be calculated as

$$\begin{bmatrix} \frac{\epsilon_{yy}}{\Omega} & -\frac{\epsilon_{xy}}{\Omega} & 0 \\ -\frac{\epsilon_{yx}}{\Omega} & \frac{\epsilon_{xx}}{\Omega} & 0 \\ 0 & 0 & \frac{1}{\epsilon_{zz}} \end{bmatrix} \begin{bmatrix} \frac{\partial H_z}{\partial y} + j\beta H_y \\ -j\beta H_x - \frac{\partial H_z}{\partial x} \\ \frac{\partial H_y}{\partial x} - \frac{\partial H_x}{\partial y} \end{bmatrix} = \begin{bmatrix} \frac{\epsilon_{yy}}{\Omega}(\frac{\partial H_z}{\partial y} + j\beta H_y) + \frac{\epsilon_{xy}}{\Omega}(j\beta H_x + \frac{\partial H_z}{\partial x}) \\ -\frac{\epsilon_{yx}}{\Omega}(\frac{\partial H_z}{\partial y} + j\beta H_y) - \frac{\epsilon_{xx}}{\Omega}(j\beta H_x + \frac{\partial H_z}{\partial x}) \\ \frac{1}{\epsilon_{zz}}(\frac{\partial H_y}{\partial x} - \frac{\partial H_x}{\partial y}) \end{bmatrix} \tag{6}$$

where $\Omega = \epsilon_{xx}\epsilon_{yy} - \epsilon_{xy}\epsilon_{yx}$.

Calculate the curl of (6) and equal the first two rows of the result to $k^2 H_x$ and $k^2 H_y$ respectively according to (5),

$$\begin{aligned} \epsilon_{yx}\beta^2 H_y + \epsilon_{xx}\beta^2 H_x =& \epsilon_{yx}(\frac{\partial^2 H_x}{\partial x \partial y} + \frac{\partial^2 H_y}{\partial y^2}) + \epsilon_{xx}(\frac{\partial^2 H_y}{\partial x \partial y} + \frac{\partial^2 H_x}{\partial x^2}) \\ & - \frac{\Omega}{\epsilon_{zz}}(\frac{\partial^2 H_y}{\partial x \partial y} - \frac{\partial^2 H_x}{\partial y^2}) + \Omega k^2 H_x \end{aligned} \tag{7a}$$

$$\begin{aligned} \epsilon_{yy}\beta^2 H_y + \epsilon_{xy}\beta^2 H_x =& \epsilon_{yy}(\frac{\partial^2 H_x}{\partial x \partial y} + \frac{\partial^2 H_y}{\partial y^2}) + \epsilon_{xy}(\frac{\partial^2 H_y}{\partial x \partial y} + \frac{\partial^2 H_x}{\partial x^2}) \\ & - \frac{\Omega}{\epsilon_{zz}}(\frac{\partial^2 H_x}{\partial x \partial y} - \frac{\partial^2 H_x}{\partial x^2}) + \Omega k^2 H_y \end{aligned} \tag{7b}$$

where from the divergence equation $\nabla \times \mathbf{B} = \nabla \times \mu_0 \mathbf{H} = 0$, longitudinal component H_z is replaced with

$$\frac{1}{j\beta}(\frac{\partial H_x}{\partial x} + \frac{\partial H_y}{\partial y}) \tag{8}$$

Solve (7) for $\beta^2 H_x$ and $\beta^2 H_y$,

$$\begin{aligned} \beta^2 H_x =& \frac{\partial^2 H_x}{\partial x^2} + \frac{\epsilon_{yy}}{\epsilon_{zz}}\frac{\partial^2 H_x}{\partial y^2} + \frac{\epsilon_{yx}}{\epsilon_{zz}}\frac{\partial^2 H_x}{\partial y \partial x} + (1 - \frac{\epsilon_{yy}}{\epsilon_{zz}})\frac{\partial^2 H_y}{\partial x \partial y} \\ & - \frac{\epsilon_{yx}}{\epsilon_{zz}}\frac{\partial^2 H_y}{\partial x^2} + k^2(\epsilon_{yy}H_x - \epsilon_{yx}H_y) \end{aligned} \tag{9a}$$

$$\begin{aligned} \beta^2 H_y =& \frac{\partial^2 H_y}{\partial y^2} + \frac{\epsilon_{xx}}{\epsilon_{zz}}\frac{\partial^2 H_y}{\partial x^2} + \frac{\epsilon_{xy}}{\epsilon_{zz}}\frac{\partial^2 H_y}{\partial x \partial y} + (1 - \frac{\epsilon_{xx}}{\epsilon_{zz}})\frac{\partial^2 H_x}{\partial y \partial x} \\ & - \frac{\epsilon_{xy}}{\epsilon_{zz}}\frac{\partial^2 H_x}{\partial y^2} + k^2(\epsilon_{xx}H_y - \epsilon_{xy}H_x) \end{aligned} \tag{9b}$$

1.2 Solve the PDE Numerically

In order to solve (9) for field components H_x and H_y and propagation constant β, a finite difference method [1] was used to approximate the partial derivatives of field components at a point as a collection of summations of field components at points surrounding it, as shown in Figure 1. Dielectric tensor $[\epsilon]$ was assumed to be homogeneous within each windows, so boundaries between materials have to coincide with grid points when generating the grid.

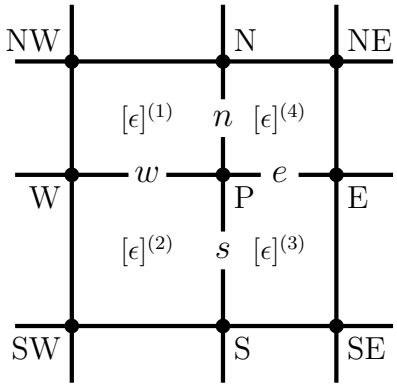

Figure 1: A sample mesh used in the finite difference method.

Applying the finite difference method, (9) can be expressed as

$$
\begin{aligned}
&a_{xx}^{(NW)}H_x^{(NW)} + a_{xx}^{(N)}H_x^{(N)} + a_{xx}^{(NE)}H_x^{(NE)} + a_{xx}^{(W)}H_x^{(W)} \\
&+ a_{xx}^{(P)}H_x^{(P)} + a_{xx}^{(E)}H_x^{(E)} + a_{xx}^{(SW)}H_x^{(SW)} + a_{xx}^{(S)}H_x^{(S)} + a_{xx}^{(SE)}H_x^{(SE)} \\
&+ a_{xy}^{(NW)}H_y^{(NW)} + a_{xy}^{(N)}H_y^{(N)} + a_{xy}^{(NE)}H_y^{(NE)} + a_{xy}^{(W)}H_y^{(W)} \\
&+ a_{xy}^{(P)}H_y^{(P)} + a_{xy}^{(E)}H_y^{(E)} + a_{xy}^{(SW)}H_y^{(SW)} + a_{xy}^{(S)}H_y^{(S)} + a_{xy}^{(SE)}H_y^{(SE)} \\
&= \beta^2 H_x^{(P)}
\end{aligned}
\tag{10a}
$$

$$
\begin{aligned}
&a_{yx}^{(NW)}H_x^{(NW)} + a_{yx}^{(N)}H_x^{(N)} + a_{yx}^{(NE)}H_x^{(NE)} + a_{yx}^{(W)}H_x^{(W)} \\
&+ a_{yx}^{(P)}H_x^{(P)} + a_{yx}^{(E)}H_x^{(E)} + a_{yx}^{(SW)}H_x^{(SW)} + a_{yx}^{(S)}H_x^{(S)} + a_{yx}^{(SE)}H_x^{(SE)} \\
&+ a_{yy}^{(NW)}H_y^{(NW)} + a_{yy}^{(N)}H_y^{(N)} + a_{yy}^{(NE)}H_y^{(NE)} + a_{yy}^{(W)}H_y^{(W)} \\
&+ a_{yy}^{(P)}H_y^{(P)} + a_{yy}^{(E)}H_y^{(E)} + a_{yy}^{(SW)}H_y^{(SW)} + a_{yy}^{(S)}H_y^{(S)} + a_{yy}^{(SE)}H_y^{(SE)} \\
&= \beta^2 H_y^{(P)}
\end{aligned}
\tag{10b}
$$

where $a_{ij}^{(K)}$s are finite difference coefficients whose expressions were given in [1]. Second order derivatives in (9) are expanded as two dimensional second order Taylor series expansion at points N, S, E and W. For each of (9), there will be a set of four equations. Each set of four equations are connected via the continuity of H_z and E_z at horizontal and vertical interfaces to form one equation that express H_x or H_y at point P as a linear sum of H_x and H_y at point P and its surrounding points.

Since (10) performs linear operations on field components, it can be rewritten in a matrix multiplication form as

$$\sum_{K=NW}^{SE} (a_{xx}^{(K)} H_x^{(K)} + a_{xy}^{(K)} H_y^{(K)}) = \sum_{K=NW}^{SE} (\begin{bmatrix} a_{xx}^{(K)} & a_{xy}^{(K)} \end{bmatrix} \begin{bmatrix} H_x^{(K)} \\ H_y^{(K)} \end{bmatrix}) = \beta^2 H_x^{(P)} \tag{11a}$$

$$\sum_{K=NW}^{SE} (a_{yx}^{(K)} H_x^{(K)} + a_{yy}^{(K)} H_y^{(K)}) = \sum_{K=NW}^{SE} (\begin{bmatrix} a_{yx}^{(K)} & a_{yy}^{(K)} \end{bmatrix} \begin{bmatrix} H_x^{(K)} \\ H_y^{(K)} \end{bmatrix}) = \beta^2 H_x^{(P)} \tag{11b}$$

Equations (11) are actually about a certain point, since field components at points surrounding it can be considered as a function of it. Apply this transformation to every point on the grid and assemble the matrices to get a global equation for the entire grid.

$$\begin{bmatrix} A_{xx} & A_{xy} \\ A_{yx} & A_{yy} \end{bmatrix} \begin{bmatrix} H_x \\ H_y \end{bmatrix} = \beta^2 \begin{bmatrix} H_x \\ H_y \end{bmatrix} \tag{12}$$

Solving (12) is to look for a nonzero vector which returns itself multiplied by a scalar after undergoing a linear transformation. Field components H_x and H_y thus form an eigenvector and β^2 is an eigenvalue of that linear transformation $\mathbf{A}$.

After transverse magnetic field components H_x and H_y and propagation constant β are found, longitudinal component H_z can be calculated from (8) and electric field components can be calculated from $\nabla \times \mathbf{H} = j\omega\mathbf{D}$ along with $\mathbf{E} = [\epsilon]^{-1}\mathbf{D}$.

2 Results

Several Python scrips were written for checking the validity of the modesolver.

2.1 Three Layer Rib Waveguide

This is a most basic example since materials are isotropic and perfectly matched layer is not applied. The profile of a basic three-layer rib waveguide is shown as

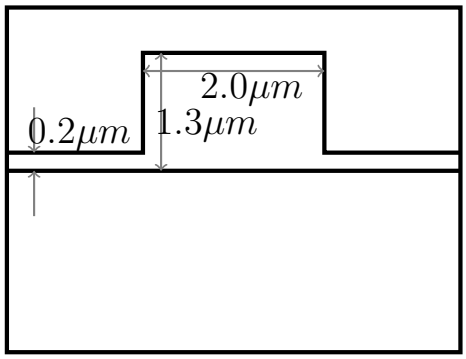

Figure 2: The profile of a three layer rib waveguide.

In this example, the refractive indices from lower cladding to upper cladding are 3.34, 3.44 and 1.00. For the fundamental TE mode, the calculated effective refractive index is 3.3886. Figure 3 are contour plots of transverse magnetic field components

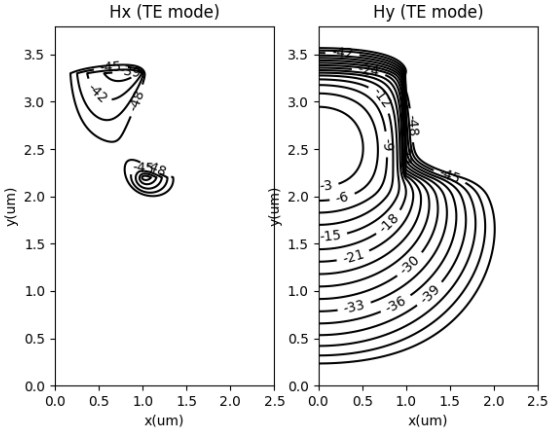

Figure 3: Fundamental TE mode.

For the fundamental TM mode, the calculated effective refractive index is 3.3878 and transverse magnetic field components were plotted as

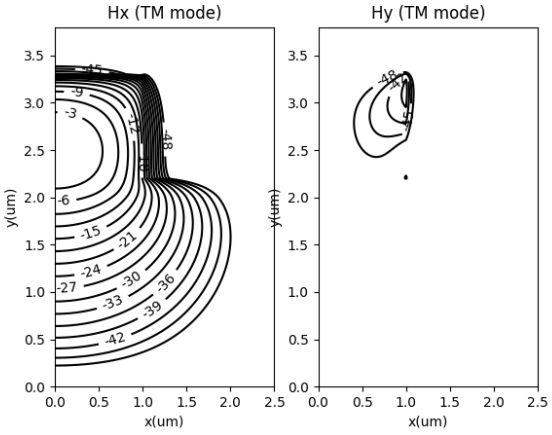

Figure 4: Fundamental TM mode.

2.2 Perfectly Matched Layer Leaky Mode

The perfect matched layer (PML) was first introduced by [2]. It suggested that when PML is applied around the computational window, it perfectly absorb any kind of wave travelling towards the edges and without any reflection.

[3] had shown that complex coordinates stretching method can be used to achieve that absorbing boundary condition. The waveguide considered here is the same as the preceding three-layer rib waveguide, with the exception that a substrate layer that has the same refractive index of the core had been added. Leaky mode occurs since the refractive index of the new substrate layer, which is 3.44 and larger than the effective refractive index of fundamental TE mode calculated in the first example (3.3886). Figure 5 shows the difference between using PML (left hand side) and not using PML (right hand side). The calculated effective refractive index is $3.3886 + j6.784 \times 10^{-5}$, a complex number, which includes the propagation loss associated with leak into the substrate.

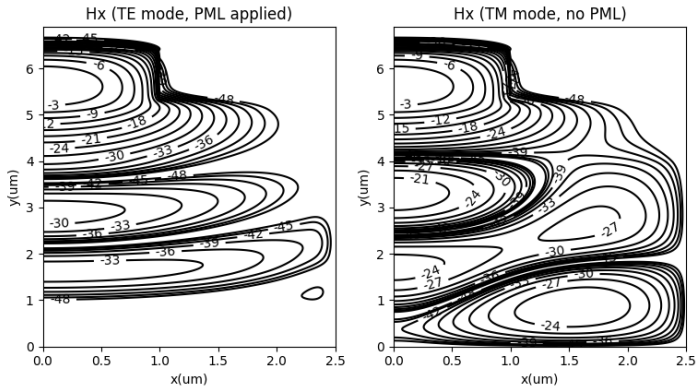

Figure 5: Fundamental TE mode for a rib waveguide in leaky mode.

2.3 Optical Fiber

This example shows the calculation of the TM_{01} mode of a step-index fiber. For the ease of implementation, only a quadrant of the fiber was taken into consideration. The calculated H_x and H_y are plotted in Figure 6 and the calculated effective refractive index is 1.8216. The exact eigenmodes was calculated by using function $jv()$, which is the Bessel function of the first kind, and $kv()$, which is the modified Bessel function of the second kind from the package *scipy.special*. The calculated H_x and H_y were plotted in Figure 7 and the calculated effective refractive index is 1.8163.

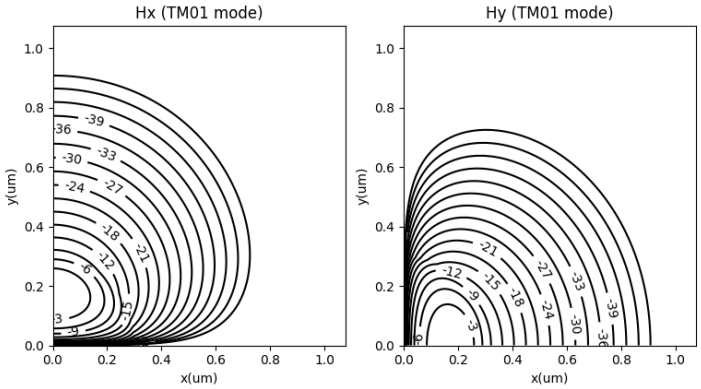

Figure 6: Solved field components H_x and H_y of TM_{01} mode.

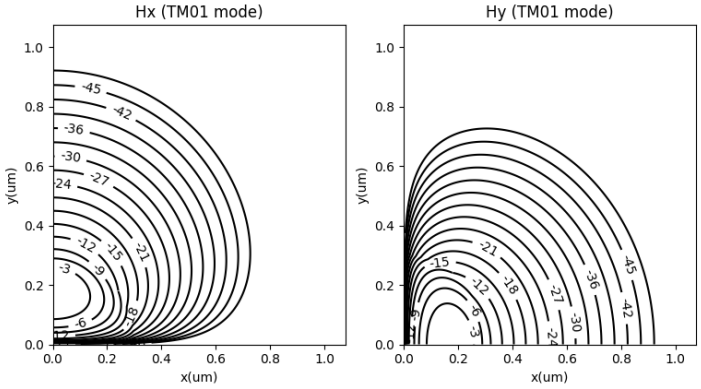

Figure 7: Exact values of field components H_x and H_y of TM_{01} mode.

2.4 Magnetooptical Channel Waveguide

This example shows the capability of modesolver for solving modes for anisotropic materials. The structure of waveguide considered here is the same as the preceding three-layer waveguide. The lower cladding layer was isotropic, with a refractive index of 1.94, the upper cladding was air, with a refractive index of 1, the core layer was anisotropic with a permittivity tensor of $\begin{bmatrix} n^2 & +j\Delta & 0 \\ -j\Delta & n^2 & 0 \\ 0 & 0 & n^2 \end{bmatrix}$, where $n = 2.18$, Faraday rotation constant

$\Delta = 2.4 \times 10^{-4}$ and a birefringence of 1.85×10^{-4}. The first two modes were calculated and plotted in Figure 8.

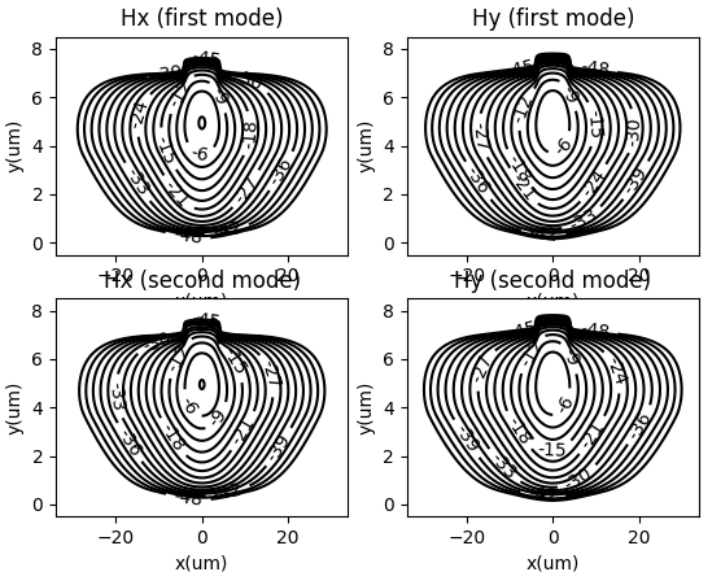

Figure 8: H_x and H_y for first two modes

For both of calculated modes, H_x and H_y are almost equal in magnitude, but out of phase by $\pm\pi/2$, indicating that the modes are circularly polarized. Figure 9 plots $(H_x + jH_y)/\sqrt{2}$ and $(H_x - jH_y)/\sqrt{2}$ for the first two modes. It can be seen that the first mode is left-hand circularly polarized and the second mode is right-hand polarized.

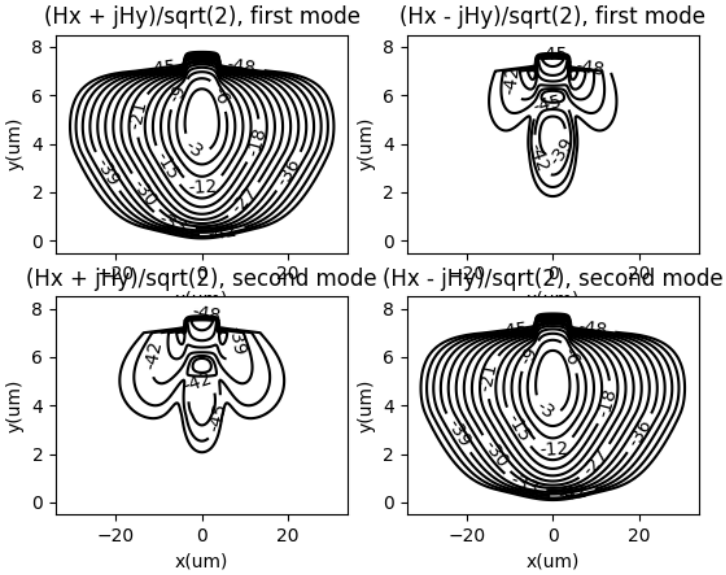

Figure 9: Circular polarized fields

References

[1] A. B. Fallahkhair, K. S. Li, and T. E. Murphy, "Vector finite difference modesolver for anisotropic dielectric waveguides," *Journal of Lightwave Technology*, vol. 26, pp. 1423–1431, June 2008.

[2] J.-P. Berenger, "A perfectly matched layer for the absorption of electromagnetic waves," *Journal of Computational Physics*, vol. 114, no. 2, pp. 185 – 200, 1994.

[3] W. C. CHEW, J. M. JIN, and E. Michielssen, "Complex coordinate stretching as a generalized absorbing boundary condition," *Microwave and Optical Technology Letters*, vol. 15, no. 6, pp. 363–369, 1997.